ISSN 1063-7761, Journal of Experimental and Theoretical Physics, 2012, Vol. 114, No. 5, pp. 810–817. © Pleiades Publishing, Inc., 2012.
Original Russian Text © A.M. Kadomtseva, G.P. Vorob'ev, Yu.F. Popov, A.P. Pyatakov, A.A. Mukhin, V.Yu. Ivanov, A.K. Zvezdin, I.A. Gudim, V.L. Temerov, L.N. Bezmaternykh, 2012, published in Zhurnal Eksperimental'noi i Teoreticheskoi Fiziki, 2012, Vol. 141, No. 5, pp. 930–938.

ORDER, DISORDER, AND PHASE TRANSITION IN CONDENSED SYSTEM

Magnetoelectric and Magnetoelastic Properties of Easy-Plane Ferroborates with a Small Ionic Radius

A. M. Kadomtseva[a], G. P. Vorob'ev[a], Yu. F. Popov[a], A. P. Pyatakov[a,b,*], A. A. Mukhin[b], V. Yu. Ivanov[b], A. K. Zvezdin[b], I. A. Gudim[c], V. L. Temerov[c], and L. N. Bezmaternykh[c]

[a] *Moscow State University, 119992 Moscow, Russia*

**e-mail: pyatakov@physics.msu.ru*

[b] *Institute of General Physics, Russian Academy of Sciences, ul. Vavilova 38, Moscow, 119991 Russia*

[c] *Kirensky Institute of Physics, Siberian Branch, Russian Academy of Sciences, Akademgorodok, Krasnoyarsk, 660036 Russia*

Received July 26, 2011

Abstract—The magnetic, magnetoelectric, and magnetoelastic properties of $RFe_3(BO_3)_4$ ferroborates are studied. The measurement of the field dependences of the magnetoelectric polarization along the *a* axis in holmium ferroborate and in the mixed composition $Ho_{0.5}Sm_{0.5}Fe_3(BO_3)_4$ revealed the following dependences for easy-plane ferroborates: (a) the longitudinal and transverse magnetoelectric effects have the opposite signs and (b) magnetically induced polarization changes its sign in a field close to the field of exchange between rare-earth and iron ions. These dependences agree well with theoretical predictions based on the symmetry of the compounds. The relatively low *f–d* exchange field in holmium ferroborate (about 20 kOe), which magnetizes the rare-earth subsystem, causes smaller polarization jumps (about 30 $\mu C/m^2$) in fields lower than 10 kOe as compared to the jumps in other easy-plane ferroborates (R = Sm, Nd). The increase in the electric polarization induced in $HoFe_3(BO_3)_4$ in magnetic fields higher than 100 kOe (200–300 $\mu C/m^2$) is found to be significantly smaller than in neodymium ferroborate, which indicates a substantial dependence of the magnetoelectric effects on the electronic structure of a rare-earth ion.

DOI: 10.1134/S1063776112030053

1. INTRODUCTION

As a new class of multiferroics, rare-earth $RFe_3(BO_3)_4$ ferroborates have been extensively studied [1–10]. The ground state of a rare-earth ion was found to affect the magnetoelectric properties of ferroborates; in particular, it was shown that easy-plane anisotropy ferroborates (Sm and Nd ferroborates) have the maximum magnetically induced polarization [3, 11, 12]. It is interesting to widen the range of the mechanisms that affect the magnetically induced polarization, in particular, its dependence on the exchange interaction between the iron subsystem and rare-earth ions, which is characterized by the *f–d* exchange field. Therefore, the purpose of this work is to measure the magnetic, magnetoelectric, and magnetoelastic properties of easy-plane $HoFe_3(BO_3)_4$ and mixed $Ho_{0.5}Sm_{0.5}Fe_3(BO_3)_4$ ferroborates, which are relatively poorly understood. These ferroborates are characterized by a variety of phase transitions, namely, structural transitions and spontaneous and magnetic field–induced spin-reorientation transitions.

2. EXPERIMENTAL

Ferroborate $HoFe_3(BO_3)_4$ and $Ho_{0.5}Sm_{0.5}Fe_3(BO_3)_4$ crystals were grown by spontaneous solidification from solutions in melts (for details, see [13]). The natural faceting of the crystals corresponded to crystallographic directions determined by X-ray diffraction. Magnetic measurements were carried out on an MPMS-5 (Quantum Design) device. The magnetic and magnetoelastic properties were measured in pulsed magnetic fields up to 250 kOe in the temperature range 4.2–50 K. Electrodes made of epoxy resin with conducting fillers were applied on the faces of a sample normal to the polarization to be measured. We measured the voltage across the electrodes, which is proportional to the electric polarization, when a magnetic field applied to various crystallographic directions was changed. The magnetostriction was measured with a piezoelectric transducer, which was made of a single-crystal quartz plate reacting to deformation in one direction and glued to a sample. The temperature dependences of the electric polarization in static magnetic fields up to 15 kOe were measured by a pyroelectric method with a B7-45 electrometer.

3. EXPERIMENTAL RESULTS

Figure 1 shows the magnetization curves of an $HoFe_3(BO_3)_4$ single crystal along the *c* and *a* axes at low temperatures (about 1.9 K) in relatively low magnetic fields. The rather sharp (especially along the *c* axis) increase in the magnetization, which is accom-

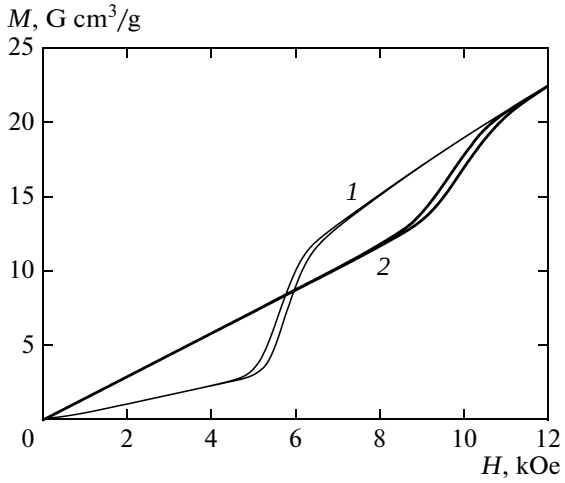

Fig. 1. Magnetization of $HoFe_3(BO_3)_4$ (*1*) along the *c* and (*2*) *a* axes at $T = 1.9$ K.

panied by a hysteresis, corresponds to the field-induced phase transition from an easy-axis to an easy-plane state (spin-flop transition). Along with the spin-flop transition, we also detected an unusual spin-reorientation transition in magnetic field **H** along axis *a* (H_a), where spins return to the *ab* plane at temperatures below the spontaneous reorientation transition ($T_{SR} \approx 5$ K, so-called re-entrant transition [1]). Such anomalies are not observed in magnetization curves at above 5 K.

Figure 2a shows the temperature dependences of the longitudinal and transverse electric polarization *P* in $HoFe_3(BO_3)_4$ that appears in low static magnetic fields (lower than 10 kOe), at which a single-domain state forms. The magnetoelectric polarization increases when the temperature decreases to the spin-reorientation phase-transition temperature ($T = 5$ K). Below this temperature, magnetoelectric polarization is not observed in low fields. Figure 2b shows the temperature dependences of longitudinal magnetoelectric polarization ΔP_a recorded for various easy-plane ferroborates in pulsed fields.

Figure 3 shows the field dependences of the longitudinal (in field H_a) and transverse (in field H_b) effects in holmium ferroborate. At low fields, we detected polarization jumps ΔP_a, which are induced by the formation of a homogeneous antiferromagnetic structure with spins oriented normal to an applied magnetic field (single-domain state). Below temperature $T_{SR} = 5$ K, a polarization jump appears in significantly higher fields (about 10 kOe), which correspond to re-entrant transition fields (Fig. 3b; Fig. 1, curve H_a). The further decrease in the magnetoelectric polarization and its vanishing in a field of 20 kOe was interpreted in [14] as the suppression of ferroelectric polarization by a magnetic field. However, the measurement of the magnetoelectric effect over a wider field range (Fig. 3) demonstrates that the sign of electric polarization changes in a field of 20 kOe, similar to the case of neodymium ferroborate in the *f–d* exchange field [3]. The sign of the transverse (at H_b) magnetoelectric effect ΔP_a is opposite to the sign of the longitudinal effect (at H_a). The latter property is characteristic of all easy-plane ferroborates, including mixed compositions (Fig. 4).

Similar features are observed in the field dependences of magnetostriction (Fig. 5), which correlate with the field dependences of polarization: a re-entrant transition is observed at 10 kOe and the sign of polarization changes in a field of 20–25 kOe, which is approximately equal to the *f–d* exchange field.

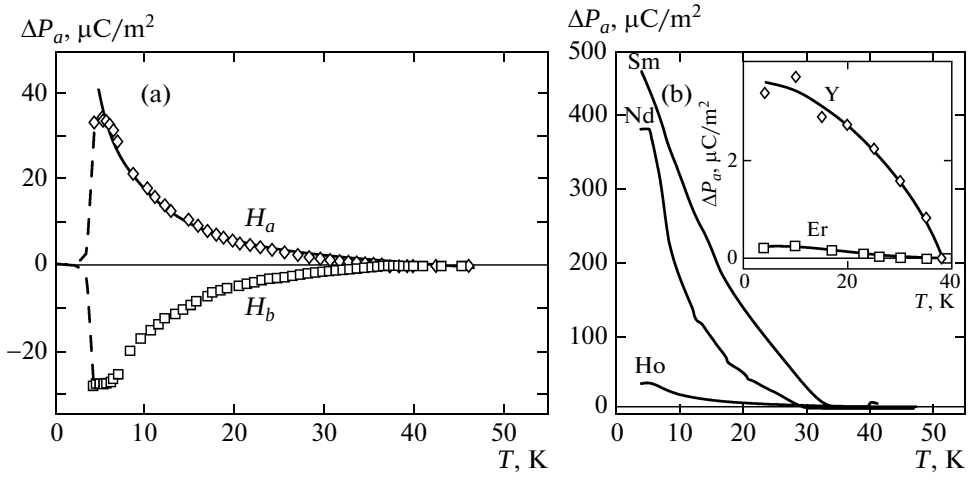

Fig. 2. Temperature dependences of magnetically induced polarization ΔP_a for (a) $HoFe_3(BO_3)_4$ in a magnetic field $H = 8.5$ kOe directed along axis *a* (H_a) or *b* (H_b). The solid curve is calculated by Eq. (3), and dashed curves show the disappearance of polarization at a temperature below $T_{SR} = 5$ K) and (b) easy-plane ferroborates R = Sm, Nd, and Ho in a field $H_a = 10$ kOe. (inset) Dependences for ferroborates with R = Er and Y.

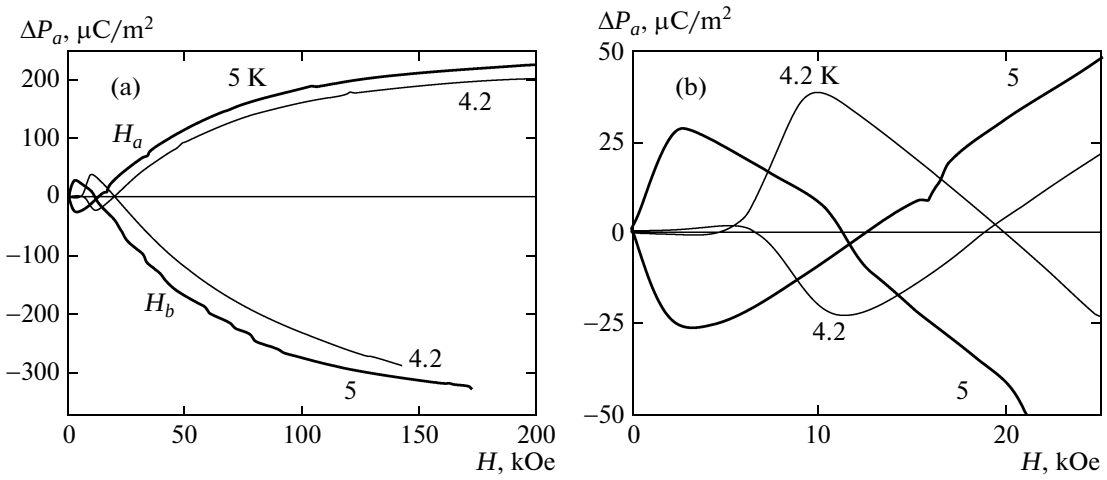

Fig. 3. (a) Electric polarization ΔP_a vs. the magnetic field directed along axis a or b in holmium ferroborate. (b) Low-field range dependence demonstrates different runs of the magnetoelectric curves above and below temperature $T_{SR} = 5$ K.

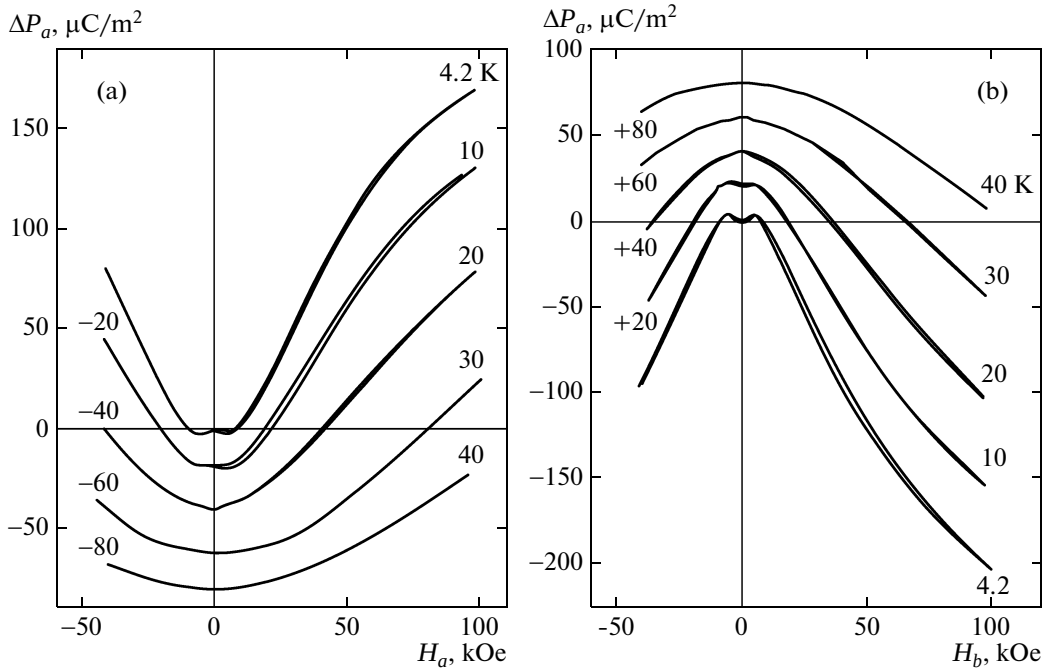

Fig. 4. Field dependences of the (a) longitudinal and (b) transverse magnetoelectric effects for the mixed composition $Ho_{0.5}Sm_{0.5}Fe_3(BO_3)_4$. For clarity, the curves at different temperatures are spaced apart (numerals at the curves indicate the shifts along the vertical axis).

Figure 6 shows the polarization of holmium ferroborate along various axes for magnetization along axis c (field H_c). The anomalies in the curves at 10 kOe have a shape characteristic of a spin-flop transition [10, 11] and are accompanied by a hysteresis similar to that in Fig. 1. The magnitude and shape of the field dependences during such a transition are mainly determined by the presence of uncontrollable magnetic field components in the basal plane.

4. DISCUSSION OF RESULTS

The field-induced spin-reorientation transition, in which the magnetic moments of iron ions return to the basal plane (re-entrant transition), is detected below the spin-reorientation temperature ($T_{SR} = 5$ K) and is similar to the transition that takes place in $GdFe_3(BO_3)_4$ at temperatures below 10 K [1]. The mechanism of this transition is related to a decrease (suppression) of the contribution of rare-earth ions to

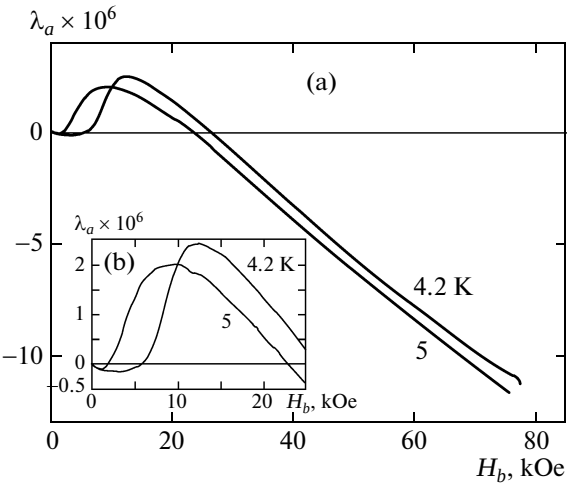

Fig. 5. (a) Field dependences of magnetostriction above and below T_{SR} for $HoFe_3(BO_3)_4$. (b) Enlarged low-field range.

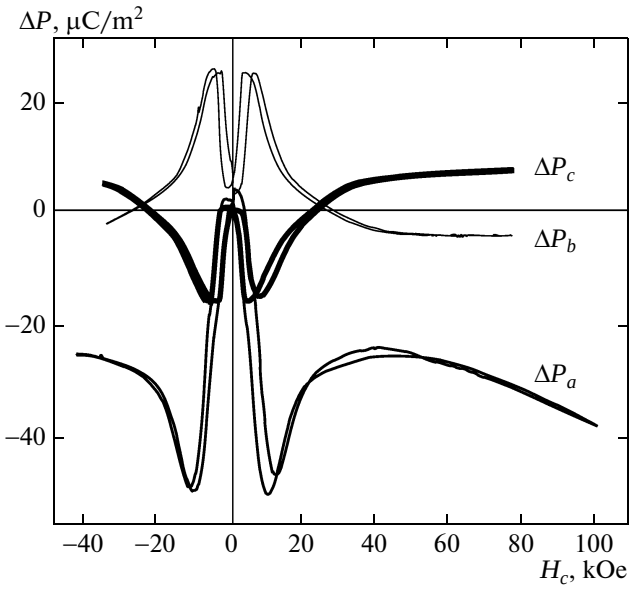

Fig. 6. Polarization in holmium ferroborate along various axes vs. the magnetic field applied along the *c* axis at $T = 4.2\ \mathrm{K} < T_{SR}$.

the anisotropy energy, which stabilizes a uniaxial state at low temperatures, in a magnetic field. The Ho^{3+} ion is characterized by the fact that its spectrum in crystal and exchange fields differs qualitatively from the equidistant spectrum of the Gd^{3+} ion [15]. However, the anisotropy of the magnetic properties of holmium ferroborate is not as high as those of terbium or dysprosium ferroborate [16, 17], where R subsystem stabilizes a uniaxial state at $T < T_N$ [8, 18, 19]. In $HoFe_3(BO_3)_4$, the contribution to the magnetic properties of four lower and closely spaced levels (0, 8, 14, 18 cm^{-1} [16]) is likely not to be strongly anisotropic; that is, specific compensation from different level pairs (transitions) takes place. This specific feature can explain a lower T_{SR} temperature than in $GdFe_3(BO_3)_4$ and a relatively weak magnetic anisotropy.

The measured field dependences of the electric polarization of ferroborate $HoFe_3(BO_3)_4$ agree well with the temperature dependences of polarization in magnetic fields up to 40 kOe obtained in [14]. However, we performed measurements over a wider magnetic-field range, including fields higher than the characteristic fields of exchange between rare-earth ions and iron ions. As a result, we were able to detect a change in the sign of magnetically induced polarization (Fig. 3b), which is characteristic of other easy-plane ferroborates [3].

To explain the specific features of the detected temperature and field dependences, we use an approach to be called a quantum-phenomenological approach. It includes both a phenomenological theory of magnetic symmetry and quantum mechanics for rare-earth elements. This method proved its extremely high efficiency upon studying a wide circle of magnetic materials [20]. We take into account that the main contribution to the electric polarization of ferroborates is related to the R subsystem, use the symmetry properties of the order parameters of the Fe and R subsystems (Table 1), and represent the magnetoelectric contribution to the free energy in the form [3]

$$\begin{aligned}\Phi_{ME}^{\mathrm{R-Fe}} &= -P_x[c_{1M}(m_xH_x^M - m_yH_y^M) \\ &+ c_{1L}(l_xH_x^L - l_yH_y^L) + c_{2M}m_yH_z^M \\ &+ c'_{2M}m_zH_y^M + c_{2L}l_yH_z^L + c'_{2L}l_zH_y^L] \\ &+ P_y[c_{1M}(m_xH_y^M + m_yH_x^M) + c_{1L}(l_xH_y^L + l_yH_x^L) \\ &+ c_{2M}m_xH_z^M + c'_{2M}m_zH_x^M \\ &+ c_{2L}l_xH_z^L + c'_{2L}l_zH_x^L],\end{aligned} \tag{1}$$

where $\mathbf{m}, \mathbf{l} = \mathbf{m}_1 \pm \mathbf{m}_2$ are the ferro- and antiferromagnetism vectors, respectively, of two R sublattices $\mathbf{m}_{1,2}$ in the effective (external $\mathbf{H}$ and exchange $\mathbf{H}^L$) field

$$\mathbf{H}_{1,2}^{\mathrm{eff}} = \mathbf{H}^M \pm \mathbf{H}^L \equiv \mathbf{H} + \hat{a}\mathbf{M} \pm \hat{b}\mathbf{L},$$

c_{1M}, c_{1L}, c_{2M}, c_{2L}, c'_{2M}, and c'_{2L} are magnetoelectric constants; $\mathbf{M}$ and $\mathbf{L}$ are the ferro- and antiferromagnetism vectors of the Fe subsystem, respectively; and $\hat{a}$ and $\hat{b}$ are the diagonal matrices of the R–Fe exchange ($a_{xx} = a_{yy} \equiv a_\perp$, $a_{zz} \equiv a_\parallel$, $b_{xx} = b_{yy} \equiv b_\perp$, $b_{zz} \equiv b_\parallel$). The existence of different magnetoelectric constants for the terms with $\mathbf{H}^M$ and $\mathbf{H}^L$ is caused by their different transformation properties under symmetry group operations.

The main contribution to the R–Fe exchange (*f*–*d* exchange) in ferroborates is determined by the isotropic part of the corresponding interaction of a

Table 1. Transformation properties of the ferro- and antiferromagnetism vectors in the Fe subsystem (**M**, **L**) and the rare-earth subsystem (**m**, **l**), polarization **P**, and strain tensor u_{ik} for ferroborates with space group $\tilde{G}_{32}$ [3] reduced from space group $R32$*

	E	T_1^-	C_3^+	2_x^+	l_i, L_i	m_i, M_i	l_iL_j	m_iM_j	P_i	u_{ij}
Γ_1	1	1	1	1	–	–	–	–	–	$u_{xx}+u_{yy}, u_{zz}$
Γ_1'	1	−1	1	1	–	–	–	–	–	–
Γ_2	1	1	1	−1	–	m_z, M_z	–	–	P_z	–
Γ_2'	1	−1	1	−1	l_z, L_z	–	–	–	–	–
Γ_3	1	1	$\mathbf{R}_3$	$\mathbf{R}_2$	–	$\begin{pmatrix} m_x \\ m_y \end{pmatrix}$, $\begin{pmatrix} M_x \\ M_y \end{pmatrix}$	$\begin{pmatrix} l_xL_x - l_yL_y \\ -l_xL_y - l_yL_x \end{pmatrix}$, $\begin{pmatrix} l_yL_z \\ -l_xL_z \end{pmatrix}$, $\begin{pmatrix} l_zL_y \\ -l_zL_x \end{pmatrix}$	$\begin{pmatrix} m_xM_x - m_yM_y \\ -m_xM_y - m_yM_x \end{pmatrix}$, $\begin{pmatrix} m_yM_z \\ -m_xM_z \end{pmatrix}$, $\begin{pmatrix} m_zM_y \\ -m_zM_x \end{pmatrix}$	$\begin{pmatrix} P_x \\ P_y \end{pmatrix}$	$\begin{pmatrix} u_{xx} - u_{yy} \\ -2u_{xy} \end{pmatrix}$, $\begin{pmatrix} u_{yx} \\ -u_{xz} \end{pmatrix}$
Γ_3'	1	−1	$\mathbf{R}_3$	$\mathbf{R}_2$	$\begin{pmatrix} l_x \\ l_y \end{pmatrix}$, $\begin{pmatrix} L_x \\ L_y \end{pmatrix}$	–	–	–	–	–

* Elements T_1^-, C_3^+, and 2_x^+ of group $\tilde{G}_{32}$ are a unit cell translation along the c axis, and rotations about the threefold and twofold axes, respectively. Superscript "+" means that a symmetry element transforms the antiferromagnetic lattice into itself. Superscript "−" means transformation into another lattice with the opposite direction of magnetization. $\mathbf{R}_2$ and $\mathbf{R}_3$ are the 180° and 120° rotation matrices, respectively. The table only gives the mixed combinations of the order parameters of Fe and R ions that contribute to polarization and strain, and the other combinations are presented in [3].

rare-earth ion in sublattices 1 and 2 with N nearest iron ions,

$$\mathcal{H}_{1,2}^{\text{fd}} = \lambda \mathbf{S}_{\text{R}}^{1,2} \sum_{i=1}^{N} \mathbf{S}_{\text{Fe}}^{i} = -\boldsymbol{\mu}_J^{1,2} \cdot \mathbf{H}_{\text{fd}}^{1,2}, \qquad (2)$$

where $\mathbf{S}_{\text{R}}$ and $\mathbf{S}_{\text{Fe}}$ are the spin moments of R and Fe ions; $\mathbf{J}_{\text{R}}$, $\boldsymbol{\mu}_J = -g_J\mu_{\text{B}}\mathbf{J}_{\text{R}}$, and g_J are the total angular moment, the magnetic moment, and the Lande factor of the ground multiplet of the R ion, respectively; μ_{B} is the Bohr magneton;

$$H_{\text{fd}} = \frac{(g_J - 1)\lambda}{g_J\mu_{\text{B}}} \sum_{i=1}^{N} S_{\text{Fe}}^{i}$$

is the f–d exchange field (isotropic part); and λ is the exchange constant, which depends on the distances and bond angles between R^{3+} and Fe^{3+} ions. This definition of the exchange field is only valid for the ground multiplet of ion R, where $\mathbf{S}_{\text{R}} \approx (g_J - 1)\mathbf{J}_{\text{R}}$ (also see [10, 12]). In the absence of an external field (when $H = 0$ and $M = 0$), exchange field $\mathbf{H}_{\text{fd}}^{1,2} = \pm\mathbf{H}^L$ is proportional to antiferromagnetism vector **L**. Assuming that constant λ weakly depends on the structural lattice parameters, we can compare the exchange fields in ferroborates with different types of rare-earth ions (Table 2) and explain the relatively low electric polarization in ferroborates with a small ionic radius in low fields, when the f–d exchange field mainly contributes to the effective field in which an ion is located. Indeed, field $|\mathbf{H}_{\text{fd}}|$ in the case of the samarium ion is higher than that of holmium by more than an order of magnitude (see Table 2).

In high magnetic fields (higher than 100 kOe), the electric polarization increases noticeably (up to 200–300 $\mu C/m^2$): it is much higher than the f–d exchange–induced polarization (Fig. 3) but is significantly lower than that in neodymium ferroborate [3]. It is obvious that this contribution is determined by the electronic structure of a rare-earth ion and its spectrum in the crystal field. The decrease in this magnetically

Table 2. *f–d* exchange fields in ferroborates depending on the type of R ion

	g_J	$\frac{g_{Gd}}{g_{Gd}-1}\frac{g_J-1}{g_J} = 2\frac{g_J-1}{g_J}$	$H_{fd}^{isotr} = 2\frac{g_J-1}{g_J}H_{fd}^{Gd}$, kOe*	$\lvert H_{fd}^{exp}\rvert$, kOe from magnetic and optical experiments	$\lvert H_{fd}^{exp}\rvert$, kOe from magnetoelectric experiments
Ce	6/7	–1/3	–23	–	–
Pr	4/5	–1/2	–35	115 [23]**	–
Nd	8/11	–3/4	–53	79 [24]	55 [3]
Pm	3/5	–4/3	–93	–	–
Sm	2/7	–5	–350	–	–
Gd	2	1	70	70 [21, 25]	–
Tb	3/2	2/3	47	35–38 [18, 24]	–
Dy	4/3	1/2	35	25 [24]	–
Ho	5/4	2/5	28	25 [26]	20
Er	6/5	1/3	23	16.5 [24]	–
Tm	7/6	2/7	20	–	–
Yb	8/7	1/4	18	–	–

* The values of H_{fd}^{isotr} (isotropic part) are calculated at $H_{fd}^{Gd} \approx 70$ kOe [21].

** The strong difference between the real exchange field acting on the Pr^{3+} ion and its isotropic part given in the fourth column is related to a high anisotropic contribution of the *f–d* exchange established for $PrFe_3(BO_3)_4$ from optical data [22].

induced contribution to polarization revealed in holmium ferroborate indicates its strong dependence on the type of rare-earth ion and, apparently, a decrease in the magnetoelectric polarization with decreasing R ion radius.

We now comprehensively consider the behavior of polarization in the easy-plane state, where a field is directed along axis *a* and vector **L** is directed along axis *b*. When minimizing the total thermodynamic potential

$$\Phi = \frac{P_x^2 + P_y^2}{2\chi_\perp^E} + \Phi_{ME}^{R-Fe}$$

with respect to polarization ($\chi_\perp^E$ is the electric susceptibility in the basal plane), we have

$$\begin{aligned} P_x &= \chi_\perp^E(c_{1M}m_x H_x^M - c_{1L}l_y H_y^L) \\ &\approx \chi_\perp^E c_{1M}\frac{m_R(H_{eff}, T)}{H_{eff}}\left(H_x^2 - \frac{c_{1L}}{c_{1M}}H_{fd}^2\right), \end{aligned} \quad (3)$$

where

$$m_R(H_{eff}, T) = -\frac{\partial \Phi_R}{\partial H_{eff}}$$

$$\equiv Nk_B T\frac{\partial}{\partial H_{eff}}\ln\sum_{i=1}^{2J+1}\exp\left(-\frac{E_i}{k_B T}\right)$$

is the magnetization of the R subsystem in the exchange field $\mathbf{H}_{eff} \approx (H_x, H_y^L, 0)$ ($H_y^L = H_{fd}$, $H_x^M \approx H_x$); its uniform and staggered components are $m_x = m_R H_x/H_{eff}$ and $m_y = m_R H_y^L/H_{eff}$, respectively; and E_i are the energy levels of ion R in the crystal and effective fields. With Eqs. (1) and (3), we can explain the following characteristic features of the temperature and field dependences in Figs. 2 and 3:

(1) the disappearance of electric polarization during the spontaneous orientation transition from the *ab* plane to the *c* axis at 5 K;

(2) the appearance of polarization during the reentrant transition to the *ab* plane induced by a field of 10 kOe;

(3) the change in the sign of electric polarization in a field of about 20 kOe, which is approximately equal to the *f–d* exchange field, at $c_{1L} \approx c_{1M}$ due to a change in the sign of the difference $c_{1M}m_x H_x - c_{1L}l_y H_y^L \sim H_x^2 - H_{fd}^2(c_{1L}/c_{1M})$ in Eq. (3); moreover, a certain difference in constants c_{1L} and c_{1M} can explain the discrepancy between the exchange fields found from the point of changing the sign of polarization during magnetic and optical measurements (see Table 2);

(4) the change in the sign of electric polarization when the magnetic field direction changes from axis *a* to axis *b* (for the same reason as in (3)).

To describe the polarization quantitatively with Eq. (3), we need the behavior of function $m_R(H_{eff}, T)$ determined by the spectrum of ion R. In the simplest two-level approximation, we have

$$m_R(H_{eff}, T) \propto \tanh(\mu_\perp H_{eff}/k_B T),$$

where $\mu_\perp$ is the magnetic moment of the R ion in the basal plane. We assume that the f–d exchange field in Eq. (3) is 20 kOe (the point of changing the sign of magnetoelectric polarization in field dependence in Fig. 3) and the applied magnetic field is $H = 8.5$ kOe (which corresponds to the experimental conditions; see Fig. 2a) and obtain the calculated temperature dependence of magnetoelectric polarization (Fig. 2a, solid line), which describes the experimental dependence rather accurately at $\mu_\perp = 2.1\mu_B$.

By analogy with Eq. (3), we obtain

$$u_{xx} - u_{yy} = (b_{3M} m_x H_x^M - b_{3L} l_y H_y^L) \approx b_{3M} \frac{m_R(H_{eff}, T)}{H_{eff}} \left(H_x^2 - \frac{b_{3L}}{b_{3M}} H_{fd}^2 \right) \quad (4)$$

for the longitudinal component of magnetostriction induced by the R subsystem. The similarity of Eqs. (3) and (4) explains the correlation of the magnetoelectric and magnetoelastic properties, and the difference in the fields of vanishing of polarization and magnetostriction can be related to the difference in coefficients c_{1L}/c_{1M} and b_{3L}/b_{3M} (see Figs. 3, 5).

5. CONCLUSIONS

Easy-plane ferroborates were shown to be characterized by the opposite signs of magnetically induced polarizations along axis a for magnetic fields directed along axes a (H_a) and b (H_b). This specific feature was explained in terms of a symmetry approach along with the change in the sign of magnetically induced polarization in a field higher than the field of exchange between rare-earth and iron ions.

The anomalies in the magnetic, magnetoelectric, and magnetoelastic dependences of holmium ferroborates are related to both a spontaneous spin-reorientation transition and magnetic field-induced (spin-flop, re-entrant) phase transitions. The field dependences of the magnetoelectric polarization measured for holmium ferroborate agree well with the similar dependences measured in [14] and substantially supplement them with the data on magnetoelectric polarization in high magnetic fields. The increase in the electric polarization in high magnetic fields in holmium ferroborate was found to be noticeably smaller than in neodymium ferroborate under these conditions, which indicates a substantial dependence of the magnetoelectric effects on the electronic structure of a rare-earth ion. A quantum-phenomenological consideration indicates that, apart from the electronic structure and magnetic moment of an rare-earth ion, the f–d exchange field is an important factor that determines the magnetoelectric polarization of rare-earth ferroborates during the rotation of a spin structure in the basal plane normal to the applied magnetic field direction in a low (less than 10 kOe) magnetic field.

ACKNOWLEDGMENTS

This work was supported by the Russian Foundation for Basic Research (project nos. 10-02-00846a, 09-02-01355, and 12-02-01261).

REFERENCES

1. A. K. Zvezdin, S. S. Krotov, A. M. Kadomtseva, G. P. Vorob'ev, Yu. F. Popov, A. P. Pyatakov, L. N. Bezmaternykh, and E. A. Popova, JETP Lett. **81** (6), 272 (2005).
2. F. Yen, B. Lorenz, Y. Y. Sun, C. W. Chu, L. N. Bezmaternykh, and A. N. Vasiliev, Phys. Rev. B: Condens. Matter **73**, 054435 (2006).
3. A. K. Zvezdin, G. P. Vorob'ev, A. M. Kadomtseva, Yu. F. Popov, A. P. Pyatakov, L. N. Bezmaternykh, A. V. Kuvardin, and E. A. Popova, JETP Lett. **83** (11), 509 (2006).
4. A. N. Vasiliev and E. A. Popova, Low Temp. Phys. **32** (8), 735 (2006).
5. M. N. Popova, E. P. Chukalina, T. N. Stanislavchuk, B. Z. Malkin, A. R. Zakirov, E. Antic-Fidancev, E. A. Popova, L. N. Bezmaternykh, and V. L. Temerov, Phys. Rev. B: Condens. Matter **75**, 224435 (2007).
6. E. A. Popova, D. V. Volkov, A. N. Vasiliev, A. A. Demidov, N. P. Kolmakova, I. A. Gudim, L. N. Bezmaternykh, N. Tristan, Yu. Skourski, B. Büchner, C. Hess, and R. Klingeler, Phys. Rev. B: Condens. Matter **75**, 224413 (2007).
7. H. Mo, Ch. S. Nelson, L. N. Bezmaternykh, and V. T. Temerov, Phys. Rev. B: Condens. Matter **78**, 214407 (2008).
8. Ch. Lee, J. Kang, K. H. Lee, and M.-H. Whangbo, Chem. Mater. **21**, 2534 (2009).
9. M. N. Popova, J. Magn. Magn. Mater. **321**, 716 (2009).
10. A. M. Kadomtseva, Yu. F. Popov, G. P. Vorob'ev, A. P. Pyatakov, S. S. Krotov, K. I. Kamilov, V. Yu. Ivanov, A. A. Mukhin, A. K. Zvezdin, A. M. Kuz'menko, L. N. Bezmaternykh, I. A. Gudim, and V. L. Temerov, Low Temp. Phys. **36** (6), 511 (2010).
11. Yu. F. Popov, A. M. Kadomtseva, G. P. Vorob'ev, A. A. Mukhin, V. Yu. Ivanov, A. M. Kuz'menko, A. S. Prokhorov, L. N. Bezmaternykh, and V. L. Temerov, JETP Lett. **89** (7), 345 (2009).
12. Yu. F. Popov, A. P. Pyatakov, A. M. Kadomtseva, G. P. Vorob'ev, A. K. Zvezdin, A. A. Mukhin, V. Yu. Ivanov, and I. A. Gudim, JETP **111** (2), 199 (2010).
13. V. L. Temerov, A. E. Sokolov, A. L. Sukhachev, A. F. Bovina, I. S. Edel'man, and A. V. Malakhovski, Crystallogr. Rep. **53** (7), 1157 (2008).
14. R. P. Chaudhury, F. Yen, B. Lorenz, Y. Y. Sun, L. N. Bezmaternykh, V. L. Temerov, and C. W. Chu, Phys. Rev. B: Condens. Matter **80**, 104424 (2009).
15. T. N. Stanislavchuk, E. P. Chukalina, M. N. Popova, L. N. Bezmaternykh, and I. A. Gudim, Phys. Lett. A **368**, 408 (2007).
16. C. Ritter, A. Vorotynov, A. Pankrats, G. Petrakovskii, V. Temerov, I. Gudim, and R. Szymczak, J. Phys.: Condens. Matter **20**, 365209 (2008).

17. A. Pankrats, G. Petrakovskii, A. Kartashev, E. Eremin, and V. Temerov, J. Phys.: Condens. Matter **21**, 436001 (2009).

18. A. K. Zvezdin, A. M. Kadomtseva, Yu. F. Popov, G. P. Vorob'ev, A. P. Pyatakov, V. Yu. Ivanov, A. M. Kuz'menko, A. A. Mukhin, L. N. Bezmaternykh, and I. A. Gudim, JETP **109** (1), 68 (2009).

19. E. A. Popova, N. Tristan, A. N. Vasiliev, V. L. Temerov, L. N. Bezmaternykh, N. Leps, B. Büchner, and R. Klingeler, Eur. Phys. J. B **62**, 123 (2008).

20. A. K. Zvezdin, V. M. Matveev, A. A. Mukhin, and A. I. Popov, *Rare-Earth Ions in Magnetically Ordered Crystals* (Nauka, Moscow, 1985) [in Russian].

21. A. M. Kadomtseva, A. K. Zvezdin, A. P. Pyatakov, A. V. Kuvardin, G. P. Vorob'ev, Yu. F. Popov, and L. N. Bezmaternykh, JETP **105** (1), 116 (2007).

22. M. N. Popova, T. N. Stanislavchuk, B. Z. Malkin, and L. N. Bezmaternykh, Phys. Rev. B: Condens. Matter **80**, 195101 (2009).

23. A. M. Kadomtseva, Yu. F. Popov, G. P. Vorob'ev, A. A. Mukhin, V. Yu. Ivanov, A. M. Kuz'menko, and L. N. Bezmaternykh, JETP Lett. **87** (1), 39 (2008).

24. M. N. Popova, J. Rare Earths **27**, 607 (2009).

25. A. M. Kuz'menko, A. A. Mukhin, V. Yu. Ivanov, A. M. Kadomtseva, and L. N. Bezmaternykh, JETP Lett. **94** (4), 294 (2011).

26. A. A. Demidov and D. V. Volkov, Phys. Solid State **53** (5), 985 (2011).

Translated by K. Shakhlevich